JOURNAL OF MATERIALS SCIENCE 33 (1998) 2413–2419

The electrochemical behaviour of direct strip casting stainless steel in acid solutions

SHYAN-LIANG CHOU, CHAO-YI LIN, JU-TUNG LEE, WEN-TA TSAI
Department of Materials Science and Engineering, National Cheng Kung University, Tainan, Taiwan
E-mail: uttsai@mail.ncku.edu.tw

The electrochemical behaviour of direct strip casting (DSC) 304 stainless steel in 0.1 M H_2SO_4 and 0.01M HCl solutions was investigated. The DSC 304 stainless steel strips were produced by using either copper-alloy roller or 304 stainless steel roller. The difference in thermal conductivity of different roller materials resulted in a change in the surface microstructure of the DSC strips. Potentiodynamic polarization curves of the DSC 304 stainless steels produced were measured in 0.1M H_2SO_4 and 0.01M HCl solutions. The results showed that both alloys could passivate in the above solutions. In the HCl solution, the passive potential range of DSC 304 stainless steel with a higher ferrite content prepared by the copper roller was wider than that with a lower ferrite content. Furthermore, the addition of silicon could cause an expansion while the addition of titanium could lead to a shrinkage in the passive range in 0.01M HCl solution. Potential decay tests in 0.1M H_2SO_4 solutions showed that the reactivation time decreased as the ferrite content was increased. © *1998 Chapman & Hall*

1. Introduction

The direct strip casting (DSC) process has many merits over the conventional steel production processes [1]. One of the most attractive advantages is cost-effectiveness. This process has been applied to produce Type 304 stainless steel strip in widths up to 330 mm and thicknesses in excess of 3 mm [2]. The success of the DSC process depends essentially upon the quality of the strips produced. Hence, product characterization was very important for the development of DSC.

Certainly, the quality of the DSC product is strongly influenced by the manufacturing process, such as melting, molten melt transfer, strip casting and post-casting treatment [3]. The variations of microstructures, phases, and mechanical properties of the DSC products with processing conditions have been the subject of many investigations [4–9]. However, only a few papers have dealt with the corrosion behaviour of DSC 304 stainless steel. Houze *et al.* [2] and Pitler [10] have investigated the corrosion property of DSC 304 stainless steel according to ASTM A262 and B117 methods. They found that the corrosion resistance of the as-cast DSC 304 stainless steel was similar to that produced by the conventional process. Obviously, more information is needed, particularly regarding the performance in various environments, before the DSC stainless steels can be widely accepted as corrosion-resistant materials.

It is known that microstructural change could greatly affect the corrosion resistance of the alloys. For DSC stainless steel, there are quite a number of factors which could cause the change of the solidification microstructure during strip casting. Among them, the uses of different cast rollers made from different materials (different thermal conductivity) could be an important factor because of the differences in cooling rate encountered. The effect of microstructural change resulting from the use of different casting rollers, on the corrosion behaviour of DSC SS is thus of interest.

In this investigation, the electrochemical behaviour of DSC 304 stainless steels, cast with rollers of different materials, in acid solutions was explored. The effect of chemical composition and microstructure on the electrochemical behaviour was studied. DSC 304 stainless steel and conventional 304 stainless steel were also compared.

2. Experimental procedure

Type 304 stainless steel strips were produced using a single-roller caster. The molten metal was prepared by melting 304 stainless steel scrap in an induction furnace with 100 kg capacity. The molten temperature at tundish was in the range 1580–1600 °C. Two types of roller were used: copper and 304 stainless steel roller, respectively. The thermal conductivity of copper is 390 $W\,m^{-1}\,K^{-1}$ while that of stainless steel is 27 $W\,m^{-1}\,K^{-1}$. Obviously, the former has a higher thermal conductivity. In both cases, the rotating speeds were all maintained at 16.8 $m\,min^{-1}$. The strips produced were about 120 mm wide by about 1.5 mm thick. The chemical compositions are listed in Table I. Samples B, D and F were prepared by employing a copper roller while samples C, E and G were obtained with a stainless steel roller. As can be seen in

TABLE I Chemical compositions (wt %) of stainless steels produced

Specimen	C	Cr	Ni	Si	Mn	P	S	Cu	Mo	V	Ti	Fe
A	0.051	19.49	8.46	0.44	1.35	0.027	0.007	0.20	0.19	0.03	–	Bal.
B	0.039	17.20	8.84	0.41	1.41	0.033	0.002	0.52	–	–	–	Bal.
C	0.035	17.40	8.92	0.40	1.32	0.029	0.002	0.52	–	–	–	Bal.
D	0.038	18.47	9.92	0.96	1.39	0.028	0.002	0.52	–	–	–	Bal.
E	0.038	18.33	9.84	0.94	1.33	0.031	0.004	0.52	–	–	–	Bal.
F	0.036	18.18	9.87	1.05	1.40	0.030	0.006	0.71	–	–	0.16	Bal.
G	0.038	18.12	9.85	1.04	1.39	0.030	0.005	0.72	–	–	0.11	Bal.

A, conventional 304 stainless steel; B, D, F, DSC stainless steel (copper roller); C, E, G, DSC stainless steel (SS roller); D, E, DSC stainless steel (silicon addition); F, G, DSC stainless steel (titanium addition).

Table I, samples D and E have higher silicon contents than samples B and C, while samples F and G are titanium containing samples.

Microstructural examination was conducted for all the 304 stainless steel strips produced. The specimens were ground with SiC paper to a grit of #1500, then polished and etched by Kalling no. 2 (5 g $CuCl_2$ + 100 ml HCl + 100 ml C_2H_5OH) solution. Surface optical micrographs were taken in three different orientations.

The specimens for electrochemical tests were cut from the middle part of the as-cast strip. The surface (lower S-plane) which was in contact with the roller was used to conduct the electrochemical test. All the specimens were ground by SiC paper to #600, washed in distilled water and rinsed in acetone before testing. Potentiodynamic polarization tests were conducted in deaerated 0.1 M H_2SO_4 and 0.01 MHCl solutions. Before conducting the experiment, the solution was purged with high-purity (99.5%) nitrogen gas for 1 h. During the measurement, high-purity nitrogen gas was also purged. An EG&G Princeton Applied Research Potentiostat/Galvanostat model 273 was used to perform potentiodynamic polarization measurement. A saturated calomel electrode (SCE) was chosen as the reference electrode. The potentiodynamic polarization curve was measured towards the anodic direction at a potential scan rate of 1 mV s^{-1}. In the potential decay measurement, each specimen was first cathodically polarized at −1500 mV for 10 min and then passivated at 400 mV for 2 h before monitoring the change of open circuit potential (OCP) in deaerated 0.1 M H_2SO_4 solution.

3. Results and discussion

3.1. Microstructural examination

The microstructures of the as-cast strips were examined. Fig. 1 shows the three-dimensional optical micrographs of samples B and C cast by different rollers. As shown in Fig. 1a, a dendritic microstructure was found in the regions close to the upper (air-cooled) and the lower (contacted with copper roller) surfaces of sample B. Vermicular structure was seen in the central region of the as-cast strip. By comparing the upper and the lower surfaces (S-plane as indicated in Fig. 1), a finer microstructure was observed for the planes in contact with and adjacent to the copper roller. The difference was attributed to the higher thermal conductivity of the copper roller as compared with air. Fig. 1b shows the microstructures of sample C, which was cast by 304 stainless steel roller. The vermicular type of microstructure was predominant with less dendritic structure located on both regions close to the surfaces. The decrease in the amount of dendritic structure in the as-cast strip of sample C was due to the low thermal conductivity of the stainless steel roller used. The dark phase was δ-ferrite as identified by X-ray diffraction analysis as shown in Fig. 2. Similar results were found for samples D, E, F and G.

More detailed examination of the change in the microstructure of the lower S-plane, which was close and adjacent to the surface in contact with the roller, with different cooling rates, were performed. Fig. 3 shows the micrographs of the lower S-planes for samples B and C. It was found that ferrite phase was much finer and distributed more uniformly in the matrix of austenite when a copper roller was used (Fig. 3a). On the other hand, when a stainless steel roller was used, ferrite was predominantly in a network form. The volume fractions of ferrite of all samples determined by using an image analyser are given in Table II. The results clearly indicate that a higher cooling rate gives rise to a higher volume fraction of ferrite of the strip in the chillzone. The additions of silicon and titanium into the stainless steel strips also caused a change in the microstructure of stainless steel. From Table II, it is seen that samples D and E had higher ferrite contents than samples B and C, and samples F and G had higher ferrite contents than samples D and E. Because silicon and titanium are ferrite stabilizers for stainless steel, the higher ferrite contents in the silicon- and titanium-containing stainless steel strips can be rationalized. Fig. 4 shows the relationship between chromium equivalent, Cr_{eq}, and ferrite content, with $Cr_{eq} = Cr + Mo + 1.5\,Si + 2\,Ti$. It is clearly shown that the ferrite content increased with increasing value of Cr_{eq} and cooling rate.

3.2. Electrochemical tests

The potentiodynamic polarization curves of various stainless steels in 0.1 M H_2SO_4 solutions are shown in Fig. 5. The results show that there is no significant difference between the conventional 304 stainless steel

(specimen A) and the DSC 304 stainless steels (specimens B, C) considering the magnitudes of passive current densities and passive ranges. The low anodic peak current densities and the higher corrosion potentials of DSC 304 stainless steels, however, indicate that they could be passivated much more easily in 0.1 M H_2SO_4 solution. It has been reported that the addition of copper (0.40%) to ferritic stainless steel could cause a decrease in the anodic peak current density in 1.0 mol dm^{-3} sulphuric acid solution [11]. As can be seen in Table I, the copper contents of the DSC stainless steels prepared in this study were higher than that of the conventional stainless steel. The lower anodic peak current densities observed for DSC stainless steels might be attributed to their higher copper content. Although the shift of corrosion potentials towards the more noble direction for DSC 304 stainless steels might result from the oxide which survived the sample preparation and cathodic polarization procedures, the enhanced passivation due to the higher copper content was more important.

Fig. 6 shows the potentiodynamic polarization curves of DSC stainless steels with different silicon content, cast with different rollers, in the 0.1 M H_2SO_4 solutions. All curves have the same features and are similar to one another. The results show that the addition of silicon as well as the cooling rate, and consequently the ferrite content, had no influence on the potentiodynamic polarization behaviour of the DSC stainless steel in 0.1 M H_2SO_4 solution. Similar results were also observed for the titanium-containing DSC stainless steels.

Fig. 7 shows the potential decay curves of different stainless steels in deaerated 0.1 M H_2SO_4 solutions. The specimens were initially held at 400 mV. After the potentiostat was turned off, the open circuit potential (OCP) of specimen B gradually decreased from 400 mV to approximately 250 mV, then suddenly decreased to about -250 mV after 235 s. For specimen C, a sharp decrease in the OCP to about -250 mV occurred after 265 s. For conventional 304 stainless steel (specimen A), however, the OCP did not fall

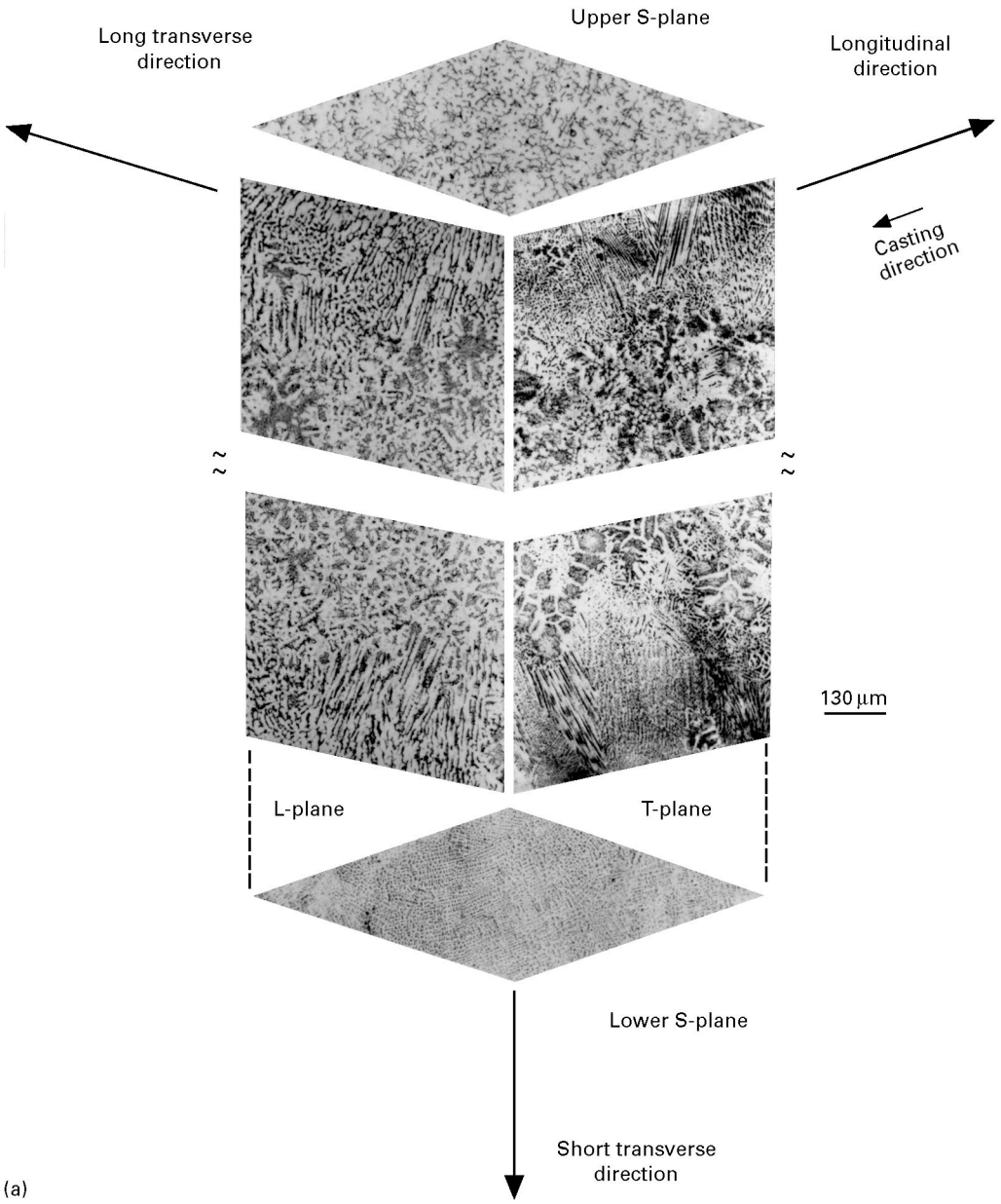

Figure 1 Three-dimensional optical micrographs of DSC stainless steels: (a) specimen B (copper roller), (b) specimen C (304 SS roller).

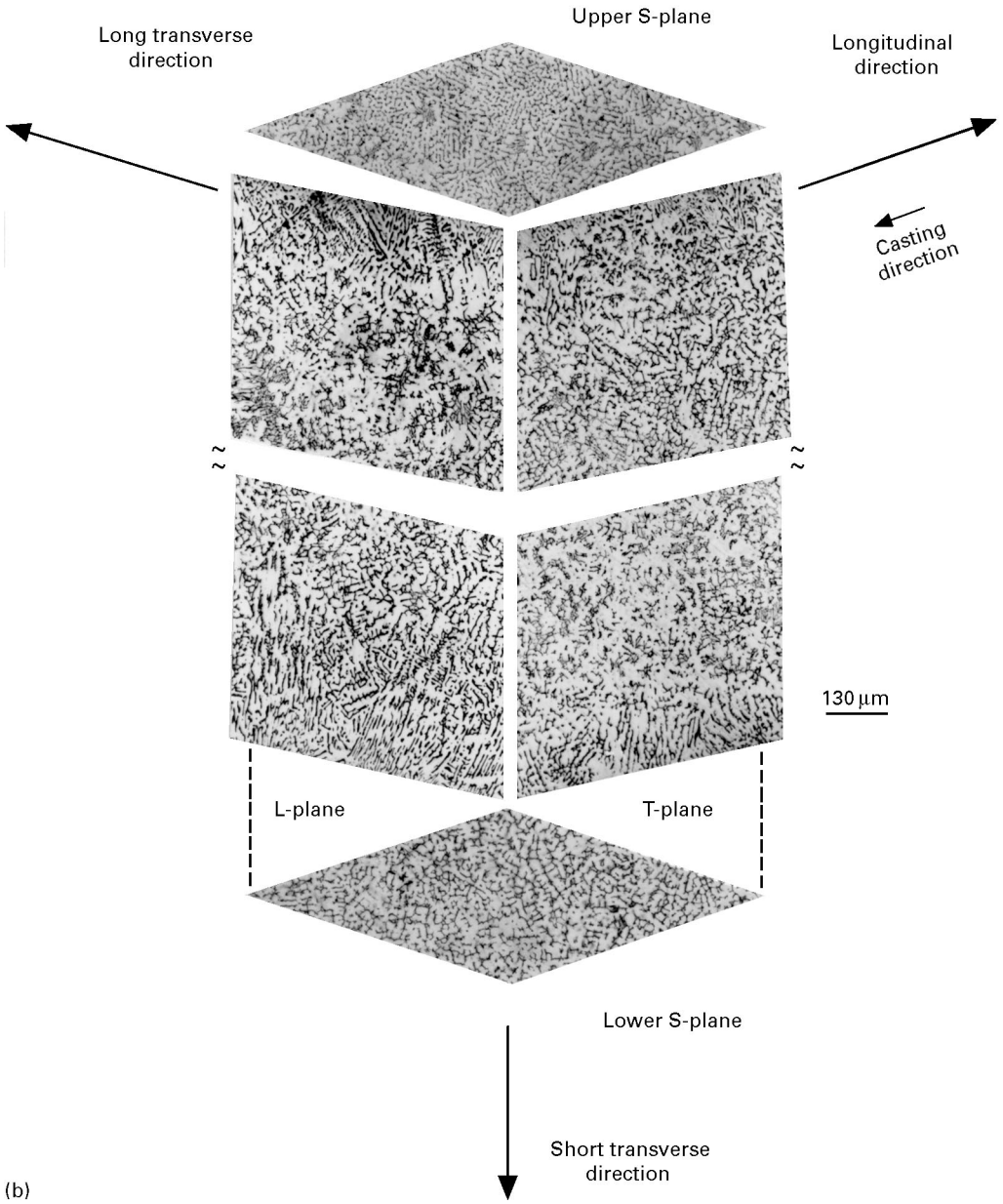

Figure 1 (continued)

sharply but decreased gradually and took 600 s to reach −120 mV. In the potential decay test, the specimen was initially held at passive potential to ensure the formation of a passive film. After the release of the applied potential, the open circuit potential tended to shift towards the active direction, due to the dissolution of the passive film in the acidic solution, until it reached a steady potential where a bare metal surface was again produced. The time required to reach this steady potential is defined as the reactivation time, τ, for the passivated stainless steel. The rate of change of the open circuit potential depends upon the stability of the passive film formed. The longer the reactivation time, the more stable is the passive film. The results shown in Fig. 7 indicate that a steady potential was never reached at 600 s for the conventional 304 stainless steel though the open circuit potential indeed decreased. Compared with the DSC 304 stainless steel specimens, the results demonstrate the passive film formed on the conventional 304 stainless steel was more stable under this particular condition. The small τ for specimen B, furthermore, reveals that the passive film formed on the DSC stainless steel produced with faster cooling rate was less stable compared with that produced with slower cooling rate. The results implied that the film stability depends on the microstructure of the stainless steel produced. The relationship between the reactivation time and the ferrite content of the DSC stainless steel is shown in Fig. 8. As can be seen in this figure, the reactivation time decreases with increasing ferrite content, except for specimen D.

The potentiodynamic polarization curves of different stainless steels in 0.01 M HCl solution are shown in Fig. 9. Pits were found in all the specimens after testing in 0.01 M HCl solution. The results show that all the stainless steels tested could be passivated in 0.01 M HCl solution with almost the same magnitude of passive current densities. But unlike those found in 0.1 M

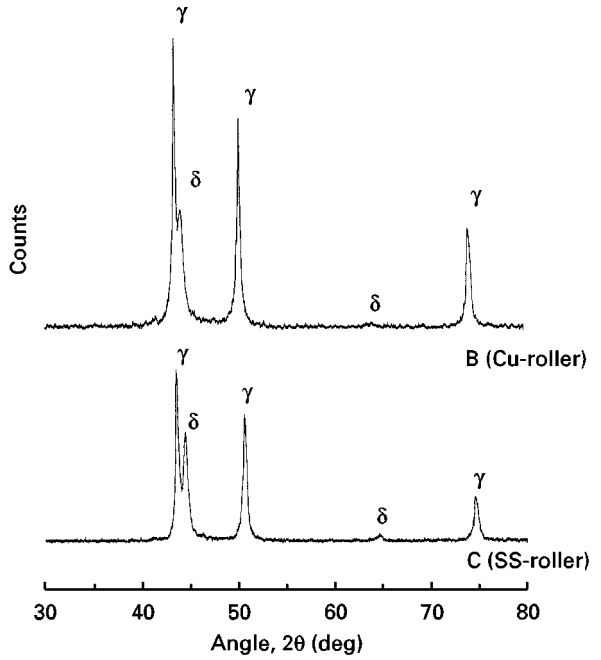

Figure 2 X-ray diffraction analysis of DSC stainless steels.

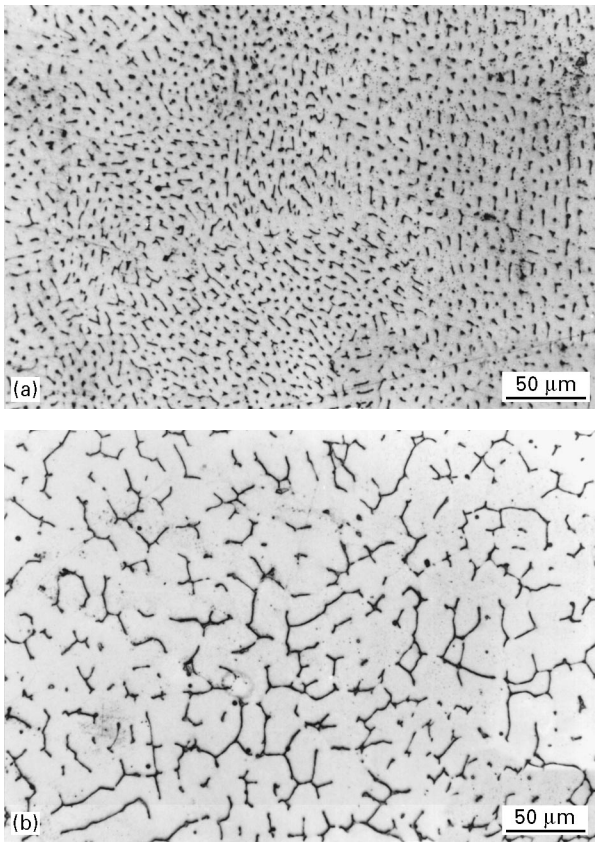

Figure 3 Micrographs of the lower S-plane: (a) specimen B (copper roller), (b) specimen C (304 SS roller).

TABLE II δ ferrite contents (vol %) of DSC stainless steels

Specimen	δ ferrite contents (vol %)
B	16.23
C	11.31
D	17.48
E	13.75
F	20.97
G	17.47

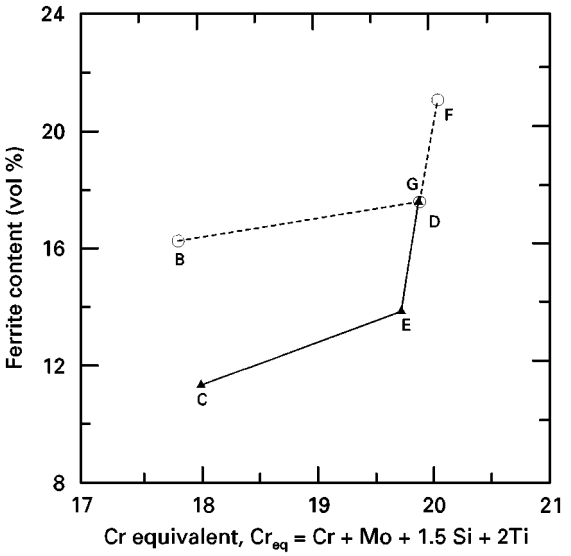

Figure 4 Relationship between Cr_{eq} and the ferrite content. (– – ○ – –) Copper roller, (—▲—) SS roller.

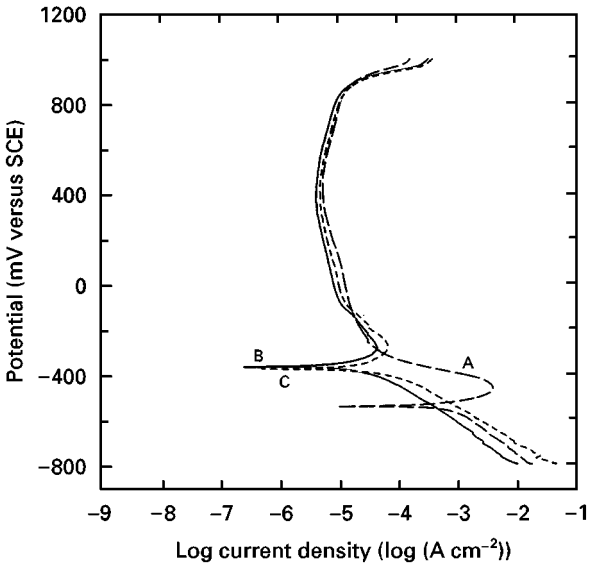

Figure 5 Potentiodynamic polarization curves of various stainless steels in 0.1 M H_2SO_4 solutions, at 25 °C. A, Conventional 304 SS; B, DSC SS (copper roller); C, DSC SS (SS roller).

H_2SO_4 solution, the passive range in 0.01 M HCl solution varied due to the different stainless steel tested. As can be seen in Fig. 9, the passive ranges of the DSC stainless steels with higher silicon contents (specimens D and E) are much wider than those with lower silicon contents (specimens B and C). Pitting corrosion was found after polarization curve measurement. The wider passive range manifested the delay in pitting corrosion. The results show that silicon could enhance the passivation of DSC stainless steels in

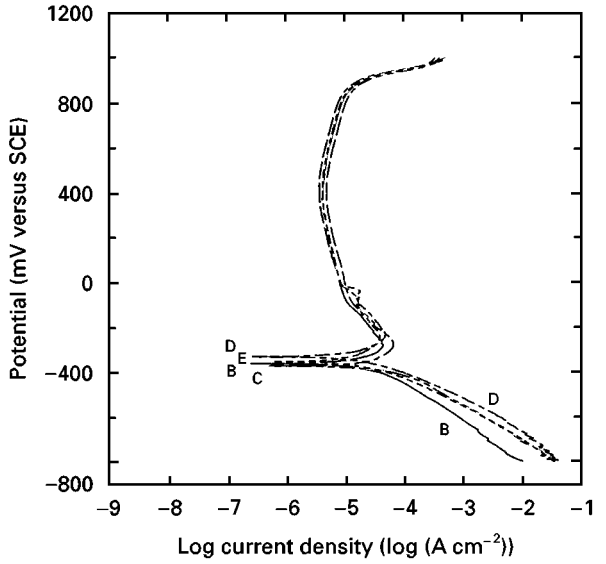

Figure 6 Potentiodynamic polarization curves of DSC stainless steels with different silicon contents in 0.1 M H_2SO_4 solutions, at 25 °C. B, Copper roller (0.41% Si); C, SS roller (0.40% Si); D, Copper roller (0.96% Si); E, SS roller (0.94% Si).

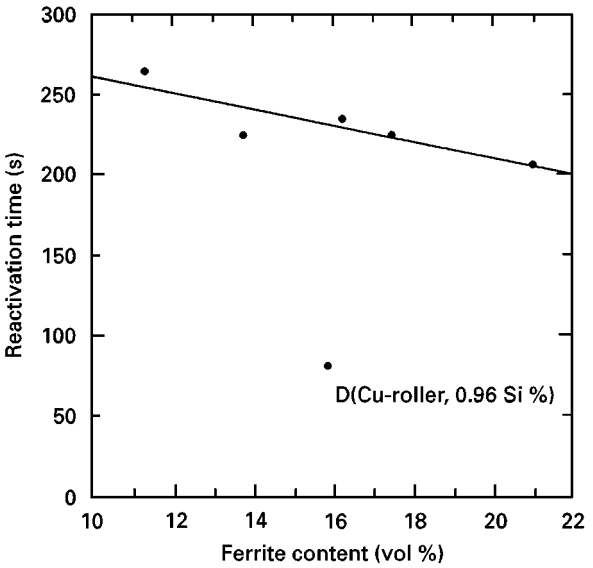

Figure 8 Relationship between reactivation time and ferrite content of DSC stainless steel. (●) D (copper roller, 0.96% Si).

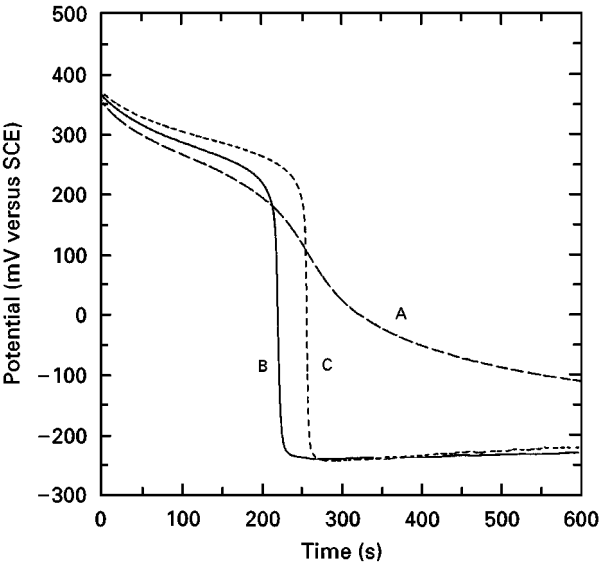

Figure 7 Potential decay curves of different stainless steels in deaerated 0.1 M H_2SO_4 solutions, for 2 h. A, Conventional 304 SS; B, DSC SS (copper roller); C, DSC SS (SS roller).

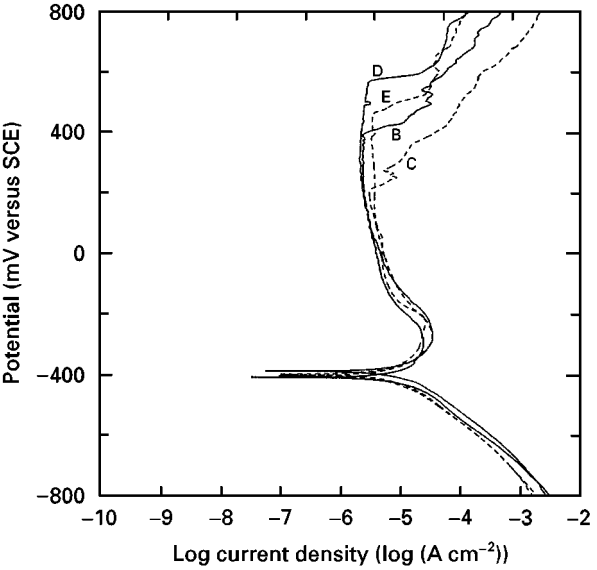

Figure 9 Potentiodynamic polarization curves of different stainless steels in 0.1 M HCl solution, at 25 °C. B, Copper roller (0.41% Si); C, SS roller (0.40% titanium Si); D, Copper roller (0.96% Si); E, SS roller (0.94% Si).

0.01 M HCl solution. It is well recognized that silicon could improve the corrosion resistance of stainless steels [12–14]. The results of this investigation further support the fact of the beneficial effect of silicon on the passivation behaviour of stainless steels. Furthermore, the results also indicate that the higher the cooling rate, the higher the pitting potential becomes. In other words, the passivation behaviour was also affected by the microstructure of the DSC stainless steels, the pitting potential increasing with increasing ferrite content. Because the ferrite phase has a higher concentration of chromium, the extension of the passive range of the DSC stainless steels with a higher ferrite content might thus be explained.

The effect of titanium addition on the potentiodynamic polarization curves of the DSC stainless steels in 0.01 M HCl solution is illustrated in Fig. 10. For specimens F and G, it can be seen that the passive ranges were smaller than those of specimens D and E. Interestingly, it is found that titanium additions of 0.11 and 0.16 wt % had an adverse effect on the electrochemical behaviour of DSC stainless steels in 0.01 M HCl. Although Srivastava and Ives [15] had ever reported the detrimental effect of titanium on the pitting resistance of stainless steels, similar to what has been observed in this study, further investigation of the corrosion behaviour of titanium-containing stainless steel in HCl solution is suggested.

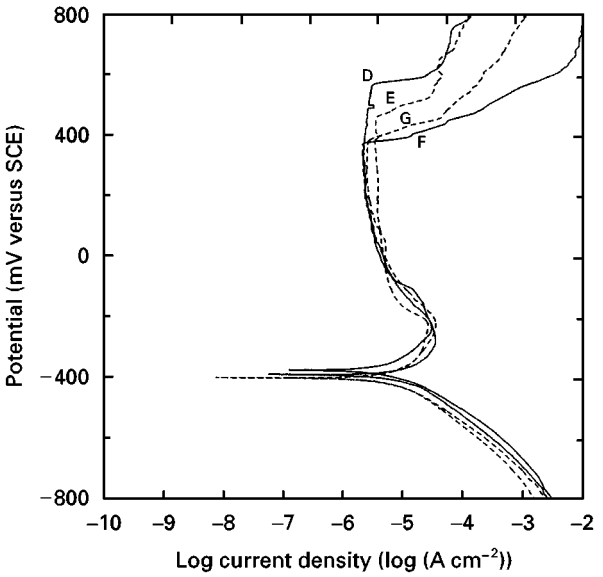

Figure 10 Effect of titanium addition on the potentiodynamic polarization curves of DSC stainless steels in 0.01 M HCl solution, at 25 °C. D, Copper roller (0.96% Si); E, SS roller (0.94% Si); F, copper roller (1.05% Si +0.16% Ti); G, SS roller (1.04% Si +0.11% Ti).

4. Conclusions

1. Duplex microstructure was found in DSC 304 stainless steels. The ferrite content in the austenite matrix increased with increasing cooling rate and with a higher contents of silicon and titanium.

2. Potential decay tests show that the stability of the passive film formed in 0.1 M H_2SO_4 solution decreased with increasing ferrite content in the DSC stainless steels tested.

3. In 0.01 M HCl solution, silicon addition could enhance the passivation by increasing the passive range. The pitting potential of the DSC stainless steels in 0.01 M HCl solution increases with increasing ferrite content (resulting from a higher cooling rate).

Acknowledgement

Financial support by the National Science Council of the Republic of China under Contract NSC 84-2216-E-006-035 is gratefully acknowledged.

References

1. K. SHIBUYA and M. OZAWA, *ISIJ Int.* **31** (1991) p. 661.
2. G. L. HOUZE, N. E. CIESLINSKI, D. B. LOVE, G. M. CARINCI and B. LINDORFER, in "VAI-Symposium", Technical Reports, Taipei, June 1993, p. 38/1.
3. R. S. CARBONARA, in "Proceedings of an International Symposium on Casting of Near Net Shape Products", edited by Y. Sahai, J. E. Battles, R. S. Carbonara and C. E. Mobley (The Metallurgical Society/AIME, Warrendale, PA, 1988) p. 169.
4. D. C. DEAN, *Iron Steelmaker* **15** (1988) p. 12.
5. T. YAMAUCHI, T. NAKANORI, M. HASEGAWA, T. YABUKI and N. OHNISHI, *Trans. Iron Steel Inst. Jpn* **28** (1988) p. 24.
6. TH. SCHUBERT, W. LOSER, S. SCHINNERLING and I. BACHER, *Mater. Sci. Technol.* **11** (1995) p. 181.
7. D. RAABE, *Metall. Mater. Trans.* **26A** (1995) p. 991.
8. T. MIZOGUCHI and K. MIYAZAWA, *ISIJ Int.* **35** (1995) 771.
9. H. YASUNAKA, K. TANIGUCHI, M. KOKITA and T. INOUE, *ibid.* **35** (1995) 784.
10. R. K. PITLER, in "Advanced High-Temperature Alloys: Processing and Properties", edited by S. M. Allen, R. Pelloux and R. Widmer (American Society for Metals, Metals Park, OH, 1986) p. 1.
11. M. SEO, G. HULTQUIST, C. LEYGRAF and N. SATO, *Corros. Sci.* **26** (1986) 949.
12. T. N. RHODIN, *Corrosion* **12** (1956) 123t.
13. B. E. WILDE, *ibid.* **42** (1986) 147.
14. W. TSAI, Y. WEN, J. LEE, H. LIOU and W. WANG, *Surf. Coat. Technol.* **34** (1986) p. 209.
15. S. C. SRIVASTAVA and M. B. IVES, *Corrosion* **45** (1989) p. 488.

Received 22 November 1996
and accepted 5 December 1997